Supporting Information

Exploring the photoswitching pathways and efficiency of NO isomerization in ethylenediamine ruthenium nitrosyl complexes

Artem A. Mikhailov[a]*, Appolinaire Tchoutchoua Tiognou[a], Anastasiya O. Brovko[b], Gennadiy A. Kostin[b], Dominik Schaniel[a]

[a] Université de Lorraine, CNRS, CRM2, UMR 7036, Nancy 54000, France b Department of Chemistry

[b] Nikolaev Institute of Inorganic Chemistry, Siberian Branch of the Russian Academy of Sciences, 3 Acad. Lavrentiev Avenue, Novosibirsk 630090, Russian Federation

*Corresponding author: artem.mikhailov.a@gmail.com

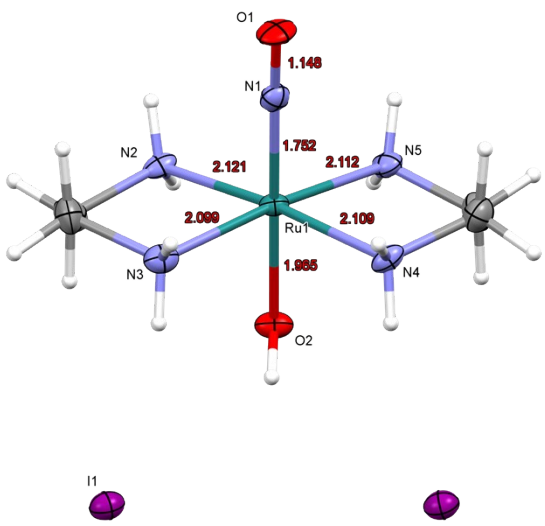

Ru-NO	1.752(8) Å
N-O	1.148(10) Å
Ru-OH	1.966(6) Å
Ru-N$_{en}$	2.110(7) Å
	2.112(8) Å
	2.099(8) Å
	2.121(7) Å
Ru-N-O	173.7(7)°

Fig. S1. Asymmetric unit of $[RuNO(en)_2OH]I_2$ structure measured at 150 K.

Table S1. Crystal data and refinement details of studied structures.

Identification code	$[RuNOen_2OH]I_2$	$[RuNOen_2OH](NO_3)_2$ (**1**, RT)
Empirical formula	$C_4H_{17}I_2N_5O_2Ru$	$C_4H_{17}N_7O_8Ru$
Formula weight	522.09	392.32
Temperature/K	150(2)	293(2)
Crystal system	monoclinic	orthorhombic
Space group	$P2_1$	Pnma
a/Å	8.3577(7)	9.2856(5)
b/Å	9.1809(7)	16.8095(6)

c/Å	9.5836(8)	8.8220(4)
α/°	90	90
β/°	110.233(2)	90
γ/°	90	90
Volume/Å^3	689.98(10)	1376.99(11)
Z	2	4
ρ_{calc}g/cm^3	2.513	1.892
μ/mm^{-1}	5.600	9.735
F(000)	484.0	792.0
Crystal size/mm^3	0.11 × 0.03 × 0.02	0.2 × 0.1 × 0.05
Radiation	MoKα (λ = 0.71073)	Cu Kα (λ = 1.54184)
2Θ range for data collection/°	5.194 to 55.034	10.526 to 152.856
Index ranges	-10 ≤ h ≤ 10, -11 ≤ k ≤ 11, 0 ≤ l ≤ 12	-9 ≤ h ≤ 10, -20 ≤ k ≤ 21, -11 ≤ l ≤ 11
Reflections collected	2971	11078
Independent reflections	2895 [R_{int} = 0.0316, R_{sigma} = 0.0282]	1431 [R_{int} = 0.0461, R_{sigma} = 0.0323]
Data/restraints/parameters	2895/1/128	1431/39/145
Goodness-of-fit on F^2	1.074	1.047
Final R indexes [I>=2σ (I)]	R_1 = 0.0355, wR_2 = 0.0903	R_1 = 0.0377, wR_2 = 0.0911
Final R indexes [all data]	R_1 = 0.0480, wR_2 = 0.0945	R_1 = 0.0486, wR_2 = 0.0997
Largest diff. peak/hole / e Å^{-3}	1.35/-1.88	0.68/-0.68
Identification code	$[RuNO(en)_2H_2O](NO_3)_3$ (**2**)	$[RuNOen_2OH](NO_3)_2$ (**1**, GS, 100 K)
Empirical formula	$C_4H_{18}N_8O_{11}Ru$	$C_4H_{15}N_7O_8Ru$
Formula weight	455.33	390.30
Temperature/K	100(1)	100(1)
Crystal system	orthorhombic	orthorhombic
Space group	$P2_12_12_1$	$P2_12_12_1$
a/Å	9.3314(2)	8.7729(2)

b/Å	11.8505(3)	9.1051(2)
c/Å	13.4342(3)	16.5461(3)
α/°	90	90
β/°	90	90
γ/°	90	90
Volume/Å^3	1485.58(6)	1321.67(5)
Z	4	4
ρ_{calc}g/cm^3	2.036	1.961
μ/mm^{-1}	1.134	1.239
F(000)	920.0	784.0
Crystal size/mm^3	0.2 × 0.1 × 0.1	0.2 × 0.1 × 0.05
Radiation	Mo Kα (λ = 0.71073)	MoKα (λ = 0.71073)
2Θ range for data collection/°	4.584 to 65.79	4.924 to 59.562
Index ranges	-14 ≤ h ≤ 13, -18 ≤ k ≤ 16, -19 ≤ l ≤ 20	-12 ≤ h ≤ 12, -12 ≤ k ≤ 12, -22 ≤ l ≤ 22
Reflections collected	28532	99184
Independent reflections	5212 [R_{int} = 0.0318, R_{sigma} = 0.0217]	3620 [R_{int} = 0.0702, R_{sigma} = 0.0211]
Data/restraints/parameters	5212/7/231	3620/0/201
Goodness-of-fit on F^2	1.033	1.038
Final R indexes [I>=2σ (I)]	R_1 = 0.0183, wR_2 = 0.0425	R_1 = 0.0309, wR_2 = 0.0687
Final R indexes [all data]	R_1 = 0.0193, wR_2 = 0.0433	R_1 = 0.0346, wR_2 = 0.0711
Largest diff. peak/hole / e Å^{-3}	0.81/-0.57	1.06/-0.69
Identification code	$[RuNOen_2OH](NO_3)_2$ (**1**, MS1, 100 K)	$[RuNOen_2OH](NO_3)_2$ (**1**, MS2, 100 K)
Empirical formula	$C_4H_{17}N_7O_8Ru$	$C_4H_{17}N_7O_8Ru$
Formula weight	392.32	392.32
Temperature/K	100(1)	100(1)
Crystal system	orthorhombic	orthorhombic

Space group	$P2_12_12_1$	$P2_12_12_1$
a/Å	8.8117(4)	8.7896(2)
b/Å	9.1391(4)	9.1067(2)
c/Å	16.4948(9)	16.5846(4)
α/°	90	90
β/°	90	90
γ/°	90	90
Volume/Å^3	1328.34(12)	1327.50(5)
Z	4	4
ρ_{calc}g/cm^3	1.962	1.963
μ/mm^{-1}	1.233	1.234
F(000)	792.0	792.0
Crystal size/mm^3	0.2 × 0.1 × 0.05	0.2 × 0.1 × 0.05
Radiation	MoKα (λ = 0.71073)	MoKα (λ = 0.71073)
2Θ range for data collection/°	4.94 to 62.202	4.912 to 62.246
Index ranges	-12 ≤ h ≤ 12, -12 ≤ k ≤ 12, -22 ≤ l ≤ 23	-12 ≤ h ≤ 12, -13 ≤ k ≤ 13, -23 ≤ l ≤ 22
Reflections collected	10892	56294
Independent reflections	3779 [R_{int} = 0.0419, R_{sigma} = 0.0564]	4156 [R_{int} = 0.0514, R_{sigma} = 0.0225]
Data/restraints/parameters	3779/2/208	4156/14/220
Goodness-of-fit on F^2	1.082	1.077
Final R indexes [I>=2σ (I)]	R_1 = 0.0369, wR_2 = 0.0753	R_1 = 0.0286, wR_2 = 0.0662
Final R indexes [all data]	R_1 = 0.0463, wR_2 = 0.0823	R_1 = 0.0324, wR_2 = 0.0689
Largest diff. peak/hole / e Å^{-3}	1.31/-0.85	1.34/-0.84
Identification code	$[(RuNOenCl_2)_2(\mu\text{-}OH)]Cl\cdot 2H_2O$ (**5**)	$[RuNO(en)_2OH](NO_3)_2\cdot 0.5AgNO_3\cdot 0.5H_2O$ (**3**)
Empirical formula	$C_4H_{21}Cl_5N_6O_5Ru_2$	$C_4H_{18}Ag_{0.5}N_{7.5}O_{10}Ru$
Formula weight	612.66	486.26

Temperature/K	100(1)	100(1)
Crystal system	monoclinic	triclinic
Space group	$P2_1/c$	P-1
a/Å	7.9938(5)	8.8973(2)
b/Å	10.5289(5)	12.8520(3)
c/Å	21.7413(12)	14.2720(3)
α/°	90	88.821(2)
β/°	90.649(5)	72.312(2)
γ/°	90	71.523(2)
Volume/Å^3	1829.76(18)	1469.49(6)
Z	4	4
ρ_{calc}g/cm^3	2.224	2.198
μ/mm^{-1}	2.407	1.783
F(000)	1200.0	968.0
Crystal size/mm^3	0.2 × 0.05 × 0.03	0.2 × 0.15 × 0.15
Radiation	Mo Kα (λ = 0.71073)	Mo Kα (λ = 0.71073)
2Θ range for data collection/°	3.746 to 61.876	3.354 to 65.87
Index ranges	-10 ≤ h ≤ 11, -14 ≤ k ≤ 9, -31 ≤ l ≤ 16	-13 ≤ h ≤ 13, -19 ≤ k ≤ 19, -21 ≤ l ≤ 21
Reflections collected	10593	46567
Independent reflections	5091 [R_{int} = 0.0384, R_{sigma} = 0.0580]	10218 [R_{int} = 0.0340, R_{sigma} = 0.0241]
Data/restraints/parameters	5091/5/225	10218/0/426
Goodness-of-fit on F^2	0.992	1.080
Final R indexes [I>=2σ (I)]	R_1 = 0.0322, wR_2 = 0.0518	R_1 = 0.0199, wR_2 = 0.0474
Final R indexes [all data]	R_1 = 0.0453, wR_2 = 0.0563	R_1 = 0.0225, wR_2 = 0.0488
Largest diff. peak/hole / e Å^{-3}	0.99/-1.05	0.67/-1.02
Identification code	$[RuNOen_2OH](NO_3)_2 \cdot H_2O$ (**4**)	
Empirical formula	$C_4H_{19}N_7O_9Ru$	

Formula weight	410.33	
Temperature/K	100(1)	
Crystal system	monoclinic	
Space group	$P2_1/n$	
a/Å	8.4249(3)	
b/Å	17.5864(5)	
c/Å	9.3788(2)	
α/°	90	
β/°	90.997(3)	
γ/°	90	
Volume/Å^3	1389.39(7)	
Z	4	
ρ_{calc}g/cm^3	1.962	
μ/mm^{-1}	1.188	
F(000)	832.0	
Crystal size/mm^3	0.2 × 0.1 × 0.05	
Radiation	Mo Kα (λ = 0.71073)	
2Θ range for data collection/°	4.632 to 52.742	
Index ranges	-10 ≤ h ≤ 10, -21 ≤ k ≤ 21, -11 ≤ l ≤ 11	
Reflections collected	43223	
Independent reflections	2838 [R_{int} = 0.0941, R_{sigma} = 0.0319]	
Data/restraints/parameters	2838/0/194	
Goodness-of-fit on F^2	1.081	
Final R indexes [I>=2σ (I)]	R_1 = 0.0271, wR_2 = 0.0590	
Final R indexes [all data]	R_1 = 0.0354, wR_2 = 0.0633	
Largest diff. peak/hole / e Å^{-3}	1.08/-0.58	

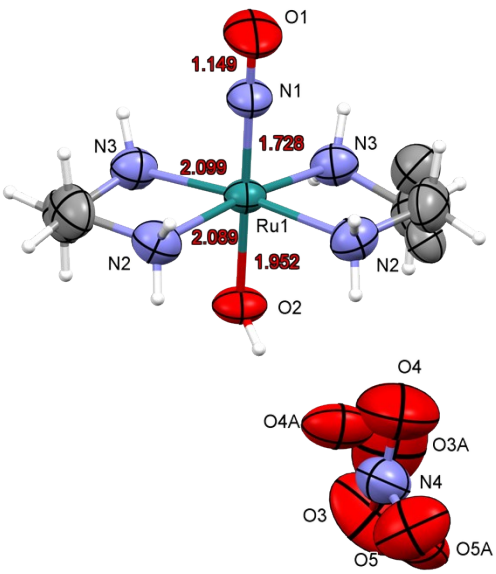

Ru-NO	1.729(5) Å
N-O	1.149(6) Å
Ru-OH	1.952(4) Å
Ru-N_{en}	2.089(3) Å
	2.089(3) Å
	2.100(4) Å
	2.100(4) Å
Ru-N-O	178.4(5)°

Fig. S2. Asymmetric unit of $[RuNO(en)_2OH](NO_3)_2$ (**1 RT**) structure measured at 300 K.

Table S2. Selected vibrational bands of **1**-**3** in GS, MS1 and MS2.

v [cm^{-1}]	GS	MS1	MS2
1	3447 (νOH) 978 (δOH) 578 (δ(Ru-N-O)/(ν(Ru-OH)) 518 (ν(Ru-NO))	3410 (νOH) 996 (δOH) 611 (ν(Ru-OH)) 500 (δ(Ru-O-N))	3358 (νOH) 1051 (δOH) 665 (δ(Ru-N-O)/(ρ(CH_2,NH_2)) 600 (ν(Ru-OH))
2	563 (ν(Ru-NO)) 552;516 (δ(Ru-N-O))	586 (ρ(H_2O)) 491 (δ(Ru-O-N))	607 (δ(Ru-N-O))
3	3451 (νOH) 977 (δOH) 578;571 (δ(Ru-N-O)/(ν(Ru-OH)) 517 (ν(Ru-NO))	3411 (νOH) 1001 (δOH) 624;610 (ν(Ru-OH)) 484 (δ(Ru-O-N))	3353 (νOH) 1047 (δOH) 668 (δ(Ru-N-O)/(ρ(CH_2,NH_2)) 605 (ν(Ru-OH))

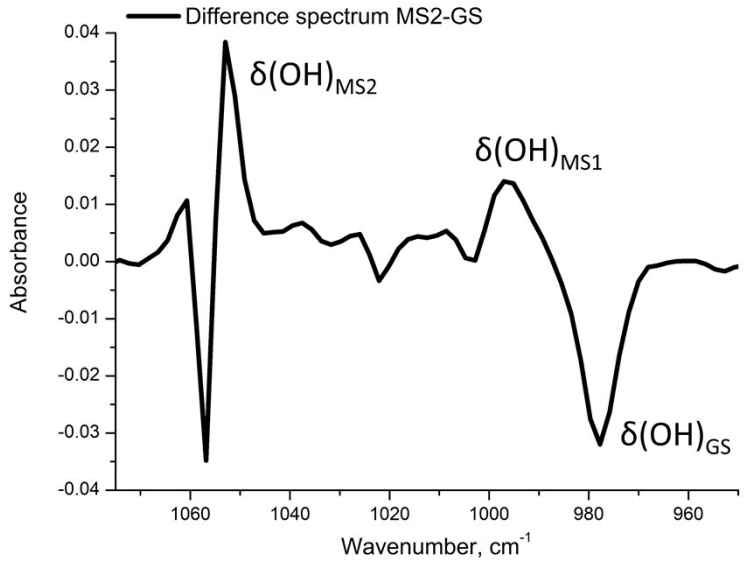

Fig. S3. Difference spectrum MS2-GS in the range of 1075-950 cm^{-1}.

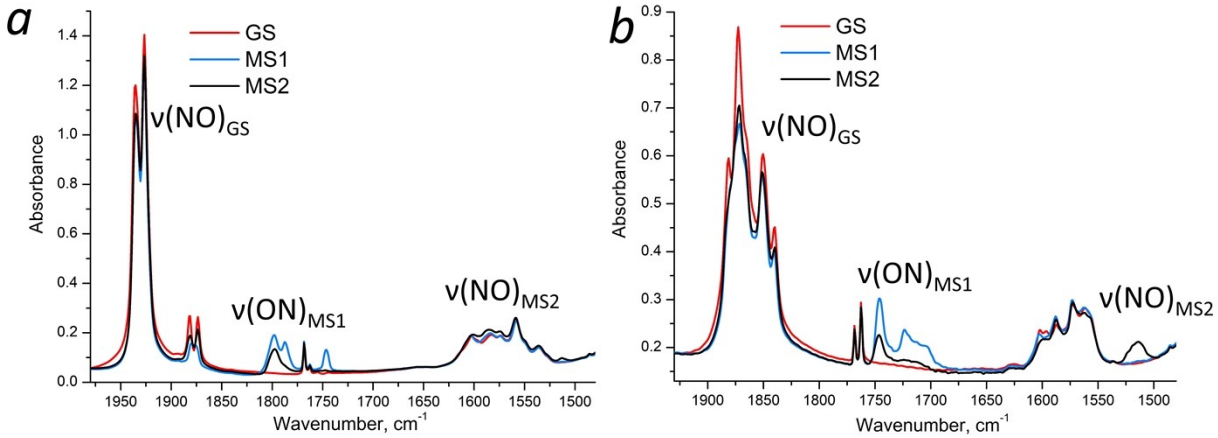

Fig. S4. IR-spectra of **2** (panel *a*) and **3** (panel *b*) in the range of 2000-1450 cm^{-1} in GS, MS1 and MS2 measured at 100 K. MS1 were generated with 420 nm light for 30 min, MS2 were produced by the subsequent irradiation of MS1 with 940 nm light for 95 and 8 min for **2** and **3**, respectively. It is important to mention that IR-spectrum of **2** comprises low intense bands of $[RuNOen_2OH]^{2+}$ complex due to partial deprotonation of H_2O ligand of **2** during the synthesis.

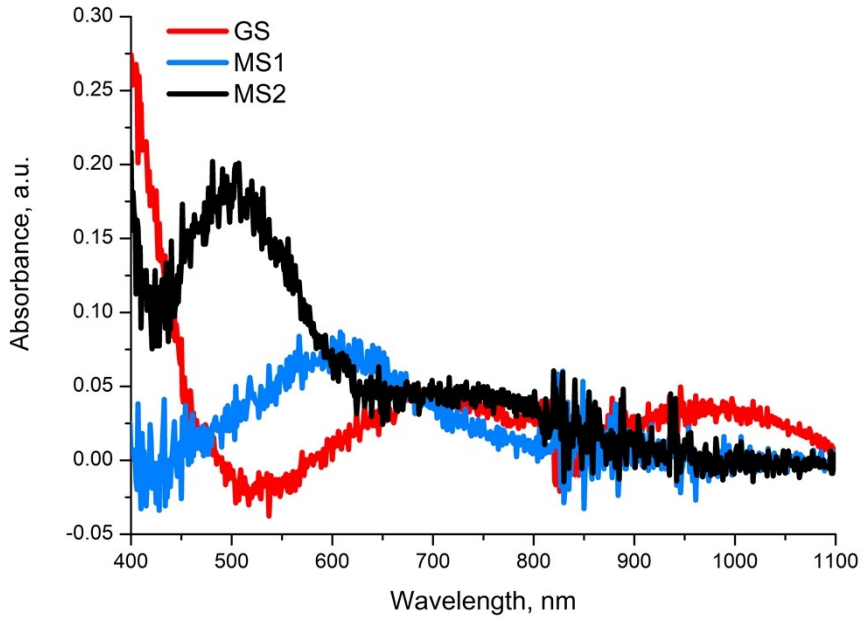

Fig. S5. UV-vis spectra of **3** in GS, MS1 and MS2 at 100 K. The spectra of MS1 and MS2 are shown as difference spectra MS1/MS2-GS. In GS the increased absorption in the range of 500-1100 nm is related to a diffusion of light caused by the KBr matrix.

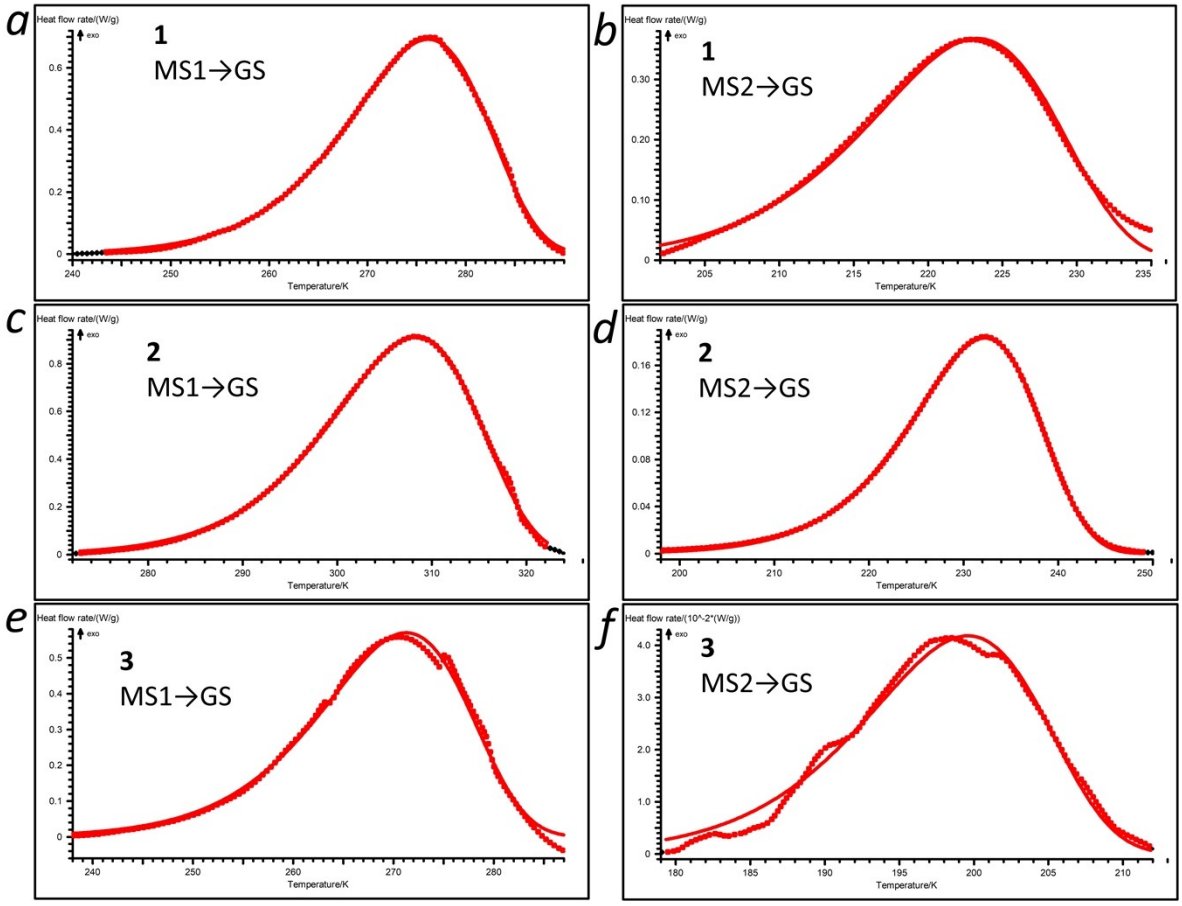

Fig. S6. DSC curves of MS1 and MS2 decay in **1** (panels *a*, *b*), **2** (panels *c*, *d*) and **3** (panels *e*, *f*).

The kinetic model details

The dependencies of IR integral absorbances for each state were described by the following scheme:

$$GS \rightleftarrows MS2 \rightleftarrows MS1,$$

with the corresponding efficient constants (J^{-1}):

$$GS \xrightarrow{k_1} MS2, \qquad MS2 \xrightarrow{k_2} GS, \qquad MS2 \xrightarrow{k_3} MS1, \qquad MS1 \xrightarrow{k_4} MS2,$$

$$\frac{dX_{GS}}{dE} = -k_1 X_{GS} + k_2 X_{MS2};$$

$$\frac{dX_{MS2}}{dE} = k_1 X_{GS} - (k_2 + k_3) X_{MS2} + k_4 X_{MS1};$$

$$\frac{dX_{MS1}}{dE} = k_3 X_{MS2} - k_4 X_{MS1}.$$

The analytical solution of the system results in the following equations for the molar fraction (X) of each state versus the irradiation energy (E).

$$X_{GS} = A_{11}C_1 + A_{21}C_2\exp(r_2E) + A_{31}C_3\exp(r_3E);$$

$$X_{MS2} = A_{12}C_1 + A_{22}C_2\exp(r_2E) + A_{32}C_3\exp(r_3E);$$

$$X_{MS1} = A_{13}C_1 + A_{23}C_2\exp(r_2E) + A_{33}C_3\exp(r_3E),$$

where r_2 and r_3 – non-zero eigenvalues of matrix:

$$\begin{matrix} -k_1 & k_2 & 0 \\ k_1 & -k_2 - k_3 & k_4 \\ 0 & k_3 & -k_4 \end{matrix}.$$

$r_2 = \frac{-a + \sqrt{a^2 - 4b}}{2}$, $r_3 = \frac{-a - \sqrt{a^2 - 4b}}{2}$, $a = k_1+k_2+k_3+k_4$, $b = k_1k_3+k_1k_4+k_2k_4$. The first eigenvalue for the matrix $r_1 = 0$.

Eigenvectors of matrix, corresponding to eigenvalues r_1-r_3:

$$\begin{matrix} A_{11} & A_{21} & A_{31} \\ A_{12} & A_{22} & A_{32} \\ A_{13}, & A_{23}, & A_{33}, \end{matrix}$$

C_1-C_3 – are coefficients determined by the initial conditions before irradiation ($E = 0$): $X_{GS} = 1$, $X_{MS1} = 0$, $X_{MS2} = 0$.

The integral absorbance of IR band is determined as $I = \varepsilon X$, where ε - integral absorption coefficient for the IR band of each isomer.

Thus, the solution of kinetic model was performed by the minimizing square deviation sum (SDS):

$$\sum (I_{GS}^{exp} - I_{GS}^{calc})^2 + (I_{MS1}^{exp} - I_{MS1}^{calc})^2 + (I_{MS2}^{exp} - I_{MS2}^{calc})^2 = f(k_1, k_2, k_3, k_4, \varepsilon_{GS}, \varepsilon_{MS1}, \varepsilon_{MS2}),$$

varying the set of k_i and ε_j.

Elimination of any reverse prosses ($k_2 = 0$ or $k_4 = 0$) results in the strong fit deviation (the SDS increases for 30 times).

Quantum yield calculation

Quantum yield (Φ) of GS→MS2 transformation was estimated using the formula considering only initial linear part of X_{GS} kinetics (X_{GS} is molar fraction of GS):

$$\Phi = \frac{k_{fit} N(GS)_0}{I_0(1 - 10^{-Aex})},$$

where k_{fit} [J^{-1}] is the slope dX_{GS}/dE_{laser} of the initial linear part of the graph (E_{laser} - total pulsed energy arrived on the sample [J]), $N(GS)_0$ [mol] initial quantity of GS molecules, I_0 [$mol \cdot J^{-1}$] is energy of 1 mol of 410 nm photons calculated by formula:

$$I_0 = \frac{\lambda_{ex}}{hcN_a},$$

where λ_{ex} [m] is wavelength of pulsed laser, h is Plank constant [J·s], c [$m \cdot s^{-1}$] – speed of light, N_a [mol^{-1}] is Avogadro number. A_{ex} is absorbance of the sample at excitation wavelength:

$$A_{ex} = \varepsilon_{ex} C_0 l_{ex},$$

where ε_{ex} [$L \cdot mol^{-1} \cdot cm^{-1}$] is absorption coefficient of GS at 410 nm, C_0 [$mol \cdot L^{-1}$] is initial concentration of GS molecules, l_{ex} [cm] – length of the light of the laser path through the sample (thickness of the sample).

Thus,

$$A_{ex} = 187.52 \cdot 0.02 \cdot 0.04 = 0.15,$$

$$I_0 = \frac{410 \cdot 10^{-9}}{6.62 \cdot 10^{-34} \cdot 3 \cdot 10^8 \cdot 6.02 \cdot 10^{23}} = 3.46 \cdot 10^{-6}\ mol \cdot J^{-1},$$

$$\Phi = \frac{0.1 \cdot 1.07 \cdot 10^{-6}}{3.46 \cdot 10^{-6} \cdot (1 - 10^{-0.15})} = 0.11\ or\ 11\%.$$